

PHYSICAL REVIEW B

CONDENSED MATTER

THIRD SERIES, VOLUME 50, NUMBER 22

1 DECEMBER 1994-II

Temperature and concentration dependences of acoustic velocity and damping in $\text{Rb}_{1-x}(\text{ND}_4)_x\text{D}_2\text{AsO}_4$ mixed crystals by Brillouin backscattering

Chi-Shun Tu and V. Hugo Schmidt

Department of Physics, Montana State University, Bozeman, Montana 59717

(Received 3 June 1994)

The LA[100] (*a*-axis) Brillouin backscattering phonon spectra have been measured as a function of temperature (20–370 K) in the mixed ferroelectric (FE)–antiferroelectric (AFE) system $\text{Rb}_{1-x}(\text{ND}_4)_x\text{D}_2\text{AsO}_4$ (DRADA-*x*) for ammonium concentrations $x=0, 0.10$, and 0.28 . The Brillouin frequency shift with decreasing temperature shows hardening (positive coupling) whose steepness decreases with higher ND_4 content. For RbD_2AsO_4 (DRDA), a Landau-Khalatnikov-like maximum (which persists in weaker form for $x=0.10$) was observed and the polarization relaxation time is estimated to be $\tau \sim 3.8 \times 10^{-12} / (T_c - T)$ s, where T_c is the ferroelectric transition temperature. For both $x=0.10$ and 0.28 , a broad damping peak anomaly which is stronger in $x=0.28$ was observed and can be connected with the dynamic order parameter fluctuations. Taking into account earlier NMR and dielectric results, we conclude that the local structure competition between FE ordering and AFE ordering is the origin of these broad damping anomalies.

I. INTRODUCTION

Since the discovery that the deuterated¹ family with the formula $A_{1-x}(\text{ND}_4)_x\text{D}_2\text{BO}_4$ [$A = \text{Rb}$ (or K) and $B = \text{P}$ (or As)] exhibits a deuteron glass state for certain values of x , similar to the proton glass state observed in the undeuterated family,^{2–5} many experimental techniques have been used in order to understand the nature of this deuterated family. In these systems, there is competition between the ferroelectric (FE) ordering and the antiferroelectric (AFE) ordering, each characterized by specific configurations of the acid protons or deuterons. The random distribution of the Rb and NH_4 (or ND_4) ions produces frustration which suppresses the long-range electric order. Spontaneous polarization revealed that RbD_2AsO_4 (DRDA) has a first-order FE transition at $T_c \sim 165$ K.⁶ Dielectric results⁶ indicated that at $T_m = 146$ K DRADA-0.10 goes from the PE (paraelectric) to a PE/FE phase coexistence region, and then to another frequency-dependent coexistence (FE-deuteron glass) region at $T_g \sim 60$ K ($f = 0.05$ MHz). Here T_m is the temperature which corresponds to the dielectric maximum. DRADA-0.28 has no FE phase but has a frequency-dependent transition from the PE to the deuteron glass phase at $T_g \sim 65$ K ($f = 0.1$ MHz).⁶ Field-heated, field-cooled, and zero-field-heated static permittivity also revealed that below $T_e \sim 38$ K (nonergodic temperature) the system enters a nonergodic state in

which on practical time scales the acid deuterons of the $\text{O-D} \cdots \text{O}$ bonds cannot rearrange sufficiently to reach all energetically allowed configurations.⁷

Earlier results of Brillouin transverse phonon spectra on mixed proton glass crystals, $\text{Rb}_{0.65}(\text{NH}_4)_{0.35}\text{H}_2\text{PO}_4$ (RADP-35),^{8,9} showed that the polarization couples linearly to the strain. In addition, Courtens *et al.* investigated the longitudinal sound waves with $q \parallel [100]$ for RADP-35 and found that the phonon modes were coupled quadratically (electrostrictively) with the linear coupling forbidden by symmetry.¹⁰ The temperature dependent of the half-width in RADP-35 exhibited a strong broad peak near 50 K that is much higher than the Vogel-Fulcher temperature $T_{\text{VF}} \sim 9$ K. These experimental data^{8–10} were analyzed assuming two contributions to the sound velocity, namely dynamic and static (space-dependent only) polarization fluctuation. This analysis led to the conclusion that a static Edward-Anderson-like order parameter¹⁰ must already exist in RADP-35 far above T_{VF} . Such a parameter is used as an indication of a system forming slow, long-range polarization fluctuations while it progresses to a glasslike state.

In principle, the acoustic coupling contributions include both static and dynamic effects.¹¹ Although the dynamic coupling always produces a negative contribution (softening) to the real part of the complex elastic stiffness change Δc^* ,¹¹ the static effect can have either sign contribution, depending on whether the phase transi-

tion is of first or second order.^{9,11,12} According to the Landau free-energy expansion with a single order parameter, the second-order transition gives a negative contribution in elastic stiffness change but the first-order can give either positive (hardening) or negative contribution for both linear and quadratic couplings.^{11,12} Several first-order examples that showed different elastic coupling behaviors can be found in Refs. 11–13.

We report here the temperature and concentration dependences of frequency shift and half-width (damping) for LA[100] phonons in mixed crystals $\text{Rb}_{1-x}(\text{ND}_4)_x\text{D}_2\text{AsO}_4$, with $x=0, 0.10$, and 0.28 from 370 to 20 K upon cooling. In particular, these results will be compared with the earlier NMR and dielectric measurements.

II. EXPERIMENTAL PROCEDURE

Single crystals of $\text{Rb}_{1-x}(\text{ND}_4)_x\text{D}_2\text{AsO}_4$ ($x=0, 0.10$, and 0.28) were grown from aqueous solutions with certain ratios of RbD_2AsO_4 (DRDA) and $\text{ND}_4\text{D}_2\text{AsO}_4$ (DADA). These crystals were carefully polished to be rectangular with average size of $1.2 \times 0.4 \times 0.2 \text{ cm}^3$. In our experiments the Brillouin spectra were obtained from backscattering geometry with scattering geometry $x(z, u)x$. Here, “ u ” means that the collection was not polarization discriminated. In order to reduce the low-lying frequency mode of the Raman spectra, we used a narrow-band (1 Å) interference filter. All samples were illuminated along the [100] phonon direction (a axis), by a Lexel Model 95-2 argon laser with $\lambda=514.5 \text{ nm}$, so the longitudinal phonons with wave vector along [100] were studied. Scattered light was analyzed by a Burleigh five-pass Fabry-Perot interferometer. To acquire more accurate data of frequency shift and half-width, the Brillouin doublets were adjusted to appear in the third order with respect to the Rayleigh line. The laser line broadening due to the jittering was claimed by the manufacturer to be about 10 MHz (half-width).¹² The laser power was kept below 100 mW. A Leybold RGD-210 closed-cycle refrigerator was used with a LakeShore DRC-91C temperature controller. The error of temperature reading was controlled to better than $\pm 0.1 \text{ K}$ and measured to $\pm 0.01 \text{ K}$ by a calibrated silicon diode thermal sensor placed on the optical sample holder. The sample was cooled from 370 down to 20 K by steps and the data were collected automatically through an analog-digital converter. Results were found to be reproducible for all three compounds.

For determination of natural-phonon half-width, the natural-phonon spectrum and the instrumental function were assumed to have Lorentz distribution, and the broadening due to collection optics was assumed to have rectangular distribution. In this case, the natural-phonon half-width W_{ph} is given by¹⁴

$$W_{\text{ph}} = (W_{\text{obs}}^2 - W_{\text{ang}}^2)^{1/2} - W_{\text{inst}}, \quad (1)$$

where W_{obs} , W_{inst} , and W_{ang} represent the observed, instrumental, and collection optical half-widths, respectively. For backscattering ($\theta=180^\circ$), W_{ang} is negligible.¹⁵ In our experiments, $W_{\text{inst}} \sim 0.02 \text{ FSR}$ where FSR is the free spectrum range obtained by measuring fused quartz.

III. RESULTS AND DISCUSSION

Actual LA[100] phonon spectra of the anti-Stokes Brillouin component are shown in Figs. 1(a)–1(c) for $x=0, 0.10$, and 0.28 , respectively. The data shown here are for several temperatures near the maximum value of half-width. The solid lines are fits of the Lorentz profile, from which the half-width W_{obs} and frequency shift can be obtained. The frequency shift temperature dependence indicates a positive coupling contribution with decreasing temperature for each compound. Comparing the half-width for different x values, we notice that the average damping value increases as ammonium concentration increases. This dependence may result from the stronger local structural FE/AFE competition that can induce larger fluctuations, especially for intermediate x values such as $0.3 \leq x \leq 0.7$ in RADP.^{1–5}

In order to estimate the coupling effect, we calculate the bare (uncoupled) phonon frequency ω_a , by fitting the frequency shift at high temperature where coupling is assumed to be negligible. The bare phonon frequency is defined as the phonon frequency in the absence of FE or AFE transition effects. The temperature dependence of ω_a can be described by a Debye anharmonic approximation as follows:^{8–10}

$$\omega_a(T, x) = \omega_a(0, x) \left[1 - A(x) \Theta(x) F \left(\frac{\Theta(x)}{T} \right) \right], \quad (2)$$

where $\Theta(x)$ is the Debye temperature, x is the ammonium concentration, $A(x)$ presents the amount of anharmonicity, $\omega_a(0, x)$ is the zero-temperature bare phonon frequency, and F is the Debye function for internal energy,¹⁶

$$F \left(\frac{\Theta}{T} \right) = \frac{3}{(\Theta/T)^4} \int_0^{\Theta/T} \frac{u^3}{e^u - 1} du \quad (3)$$

as tabulated, for example, by Abramowitz and Stegun.¹⁷

The temperature dependences of the Brillouin shift and half-width for $x=0, 0.10$, and 0.28 are shown in Figs. 2–4, respectively. The solid lines in frequency shift are the calculations of Eq. (2) with parameters of Table I. Those parameters A , $\omega_a(T=0)$, and Θ of Table I are from the fits of Eq. (2) to the high temperature ($\geq 270 \text{ K}$) measured values of the Brillouin shift. Here we assume that temperatures above 270 K are far above the coupled region since all phase transitions occur below 200 K. One finds that Θ and $\omega_a(0, x)$ tend to increase from the DRDA side to the DADA side, as expected in view of the higher frequency of the modes on the DADA-rich side.¹⁶ Also, the anharmonic factor A increases with considerably higher ND_4 content.

Figure 2 for $x=0$ (pure DRDA) shows a sharp damping peak at 164.8 K associated with an upward step in frequency which is expected, since the KH_2PO_4 (KDP) family has linear $\eta\mu$ -type piezoelectric coupling.^{11,14} Here η is the order parameter and μ is the strain. Such a sharp damping maximum for longitudinal acoustic phonons can be connected with the Landau-Khalatnikov relaxation-type mechanism.^{11,14} The dashed line in half-width of Fig. 2 is a qualitative estimate for this relaxa-

tion portion. We also try to estimate the pure lattice-anharmonic contribution by solid circles, which is the typical anharmonic half-width observed in Brillouin scattering for dielectrics.^{10,18} For linear coupling with the assumption of a single relaxation time, the sound velocity and the attenuation α in the FE phase can be given by¹⁴

$$V^2 = V_\infty^2 - \frac{V_\infty^2 - V_0^2}{1 + \omega^2 \tau_0^2 t^{-2}}, \quad (4)$$

$$\alpha = \frac{\omega^2 \tau_0 t^{-1}}{2V^3} \frac{V_\infty^2 - V_0^2}{1 + \omega^2 \tau_0^2 t^{-2}}, \quad (5)$$

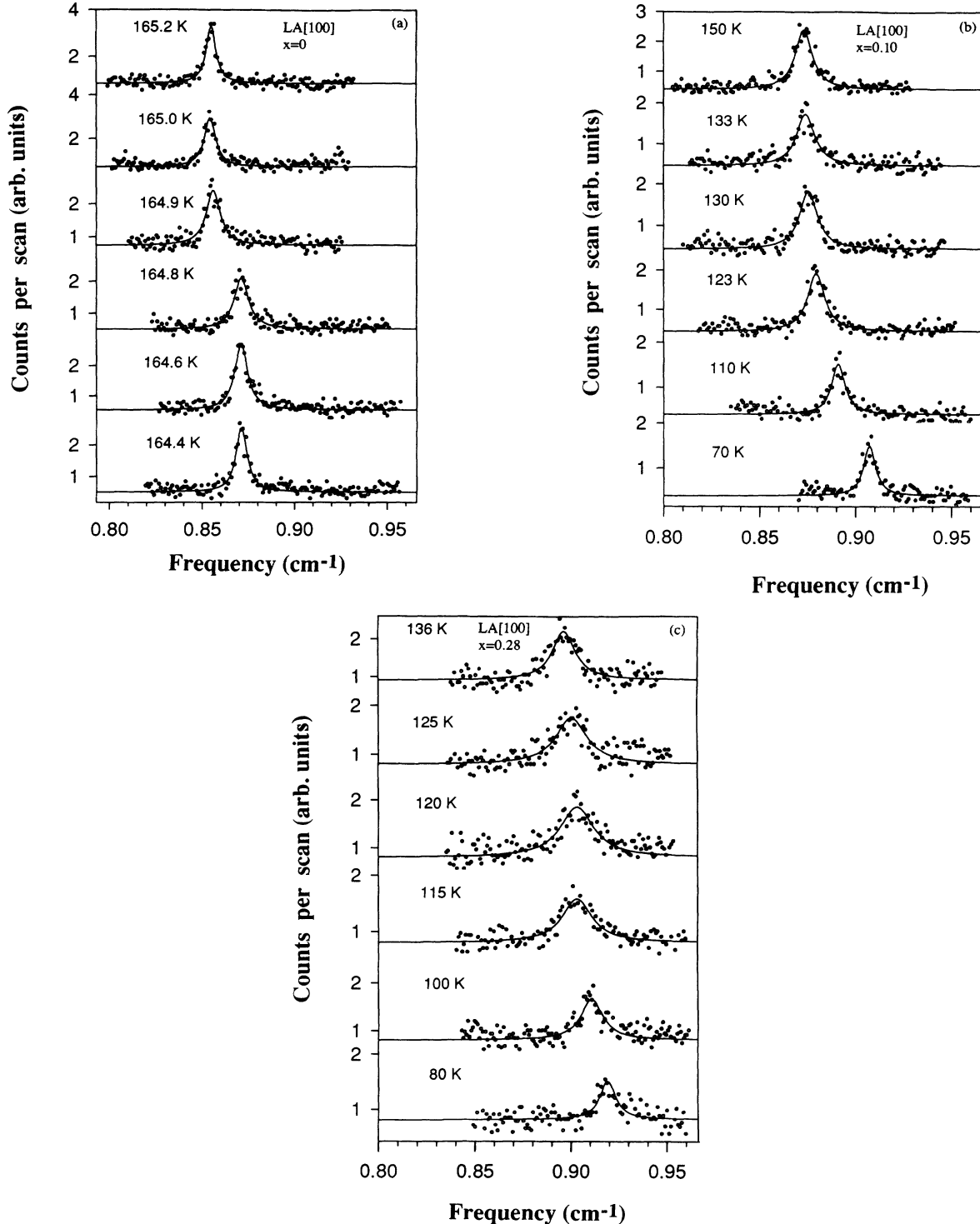


FIG. 1. Anti-Stokes components of the LA[100] Brillouin frequency shift for temperatures around the maximum value of half-width for (a) $x=0$ (DRDA), (b) $x=0.10$, and (c) $x=0.28$. The open circles are the measured data and solid lines are the Lorentz fits.

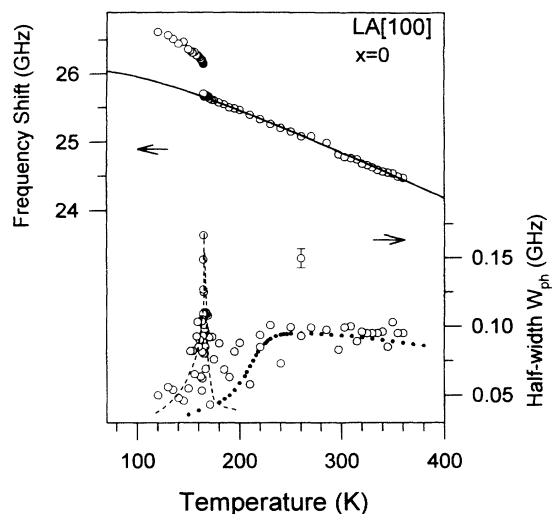


FIG. 2. Frequency shift and half-width vs temperature of the LA[100] phonons for $x = 0$ (DRDA). The solid line for frequency shift is the Debye anharmonic calculation with parameters from Table I. The dashed line and solid circles for half-width are the qualitative estimates for the Landau-Khalatnikov and pure lattice anharmonic contributions, respectively. The error bar indicates the error range for the half-width experimental points.

where t is the reduced temperature $(T_c - T)/T_c$, and τ_0 is the elementary individual-dipole relaxation time in the expression $\tau = \tau_0 t^{-1}$ for the relaxation time τ . The velocities V_∞ and V_0 designate the high- and low-frequency limit velocities, respectively. From Eqs. (4) and (5) we can obtain the relation¹⁴

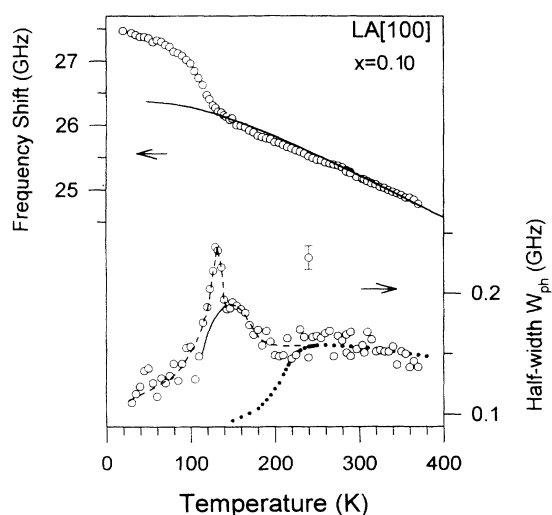


FIG. 3. Frequency shift and half-width vs temperature of the LA[100] phonons for $x = 0.10$. The solid line for frequency shift is the Debye anharmonic calculation with parameters from Table I. The solid line and solid circles for half-width are the estimates of fluctuations and pure lattice anharmonic contributions, respectively. The dashed line is a guide to the eye. The error bar indicates the error range for the half-width experimental points.

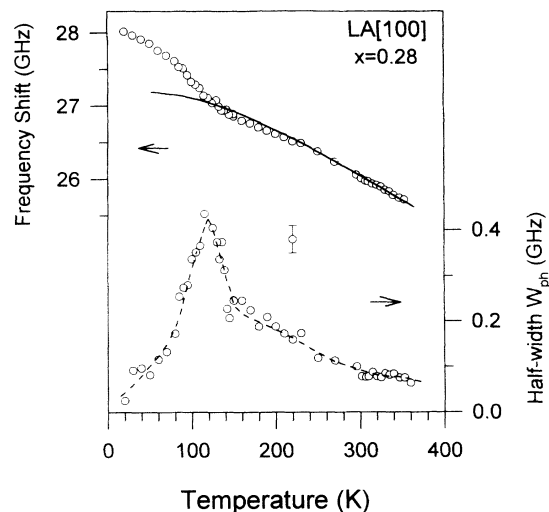


FIG. 4. Frequency shift and half-width vs temperature of the LA[100] phonons for $x = 0.28$. The solid line for frequency shift is the Debye anharmonic calculation with parameters from Table I. The dashed line is a guide to the eye. The error bar indicates the error range for the half-width experimental points.

$$\omega\tau_0 = \frac{T_c - T_m}{T_c} \quad (6)$$

By this relation we can calculate the elementary relaxation time τ_0 . Here, $T_m = 164.8$ K is the temperature at which the half-width is maximum and the FE transition temperature T_c is defined as the point at which the frequency shift curve is steepest. For the LA[100] phonons of DRDA, we obtain the following result:

$$\begin{aligned} T_c - T_m &\sim 0.1 \text{ K}, \\ \tau_0 &\sim 2.3 \times 10^{-14} \text{ s}, \\ \tau &\sim \frac{3.8 \times 10^{-12}}{T_c - T} \text{ s}. \end{aligned}$$

The elementary dipole relaxation time τ_0 obtained from the LA[100] phonons of DRDA is short compared to that of the other order-disorder ferroelectrics. For instance, τ_0 is 1.2×10^{-13} s for potassium dihydrogen phosphate¹⁴ (KDP) and 1.3×10^{-12} s for deuterated potassium dihydrogen phosphate (DKDP).¹⁴

Instead of a sharp peak, the damping data of Fig. 3 for $x = 0.10$ exhibits a smooth growth from ~ 200 down to ~ 130 K, associated with a slowly rising anomaly in frequency shift above the Debye curve of Eq. (2). Such an increasing of damping which begins far above $T_m = 146$

TABLE I. Parameters from the fits of Eq. (2) to high-temperature measured values of frequency shift.

	$\omega_a(T=0)$ (GHz)	A (K^{-1})	Θ (K)
DRDA	26.08	2.70×10^{-4}	400
DRADA-0.10	26.37	2.76×10^{-4}	480
DRADA-0.28	27.20	2.84×10^{-4}	520

K must be associated with the order parameter fluctuations.¹¹ A qualitative estimate of this fluctuation contribution is given by the solid curve in Fig. 3 with maximum near 146 K. Beside this broad damping background, one can note that there is an additional peak appearing near 130 K that can be connected with the Landau-Khalatnikov maximum.

What are the origins of these two damping maxima in DRADA-0.10? The ND_4^+ deuteron NMR spectra¹⁹ of DRADA-0.10 showed a gradual disappearance of the doublet near 131 K where the single broad linewidth grows to its full size, from which it was concluded that below 131 K the FE phase portion is greater than PE in the crystal and becomes the dominant ordering. This result is consistent with the presence of PE/FE phase coexistence as evidenced by dielectric results which show that a gradual ferroelectric transition begins at $T_m = 146$ K and is mostly completed at ~ 120 K.⁶ Furthermore, the real part of dielectric permittivity $\epsilon_{11}(T)$ shows deviation from the Curie-Weiss law below 160 K.⁶ This high-temperature dielectric anomaly below 160 K can be associated with the onset of short-range antiferroelectric order due to the freezing-in of the ND_4 reorientations² and implies a growth of local structural competition (between FE and AFE ordering). On the whole, one can expect that such FE/AFE ordering competition, which can suppress a long-range-order ferroelectric transition and generate the order parameter fluctuations, is responsible for both FE/PE phase coexistence and development of the broad damping peak centered at ~ 146 K. Also, the rapid growth of FE ordering near 130 K is the origin of the Landau-Khalatnikov-like maximum in DRADA-0.10.

An even stronger damping temperature dependence which shows a growth from ~ 300 down to ~ 120 K (see Fig. 4) is observed for $x = 0.28$, associated with a smoothly rising frequency shift. This strong broad damping reveals that fluctuations are the dominant dynamic mechanism. As one knows,¹¹ the dynamic fluctuation contribution for longitudinal acoustic phonons is a characteristic of an $\eta^2\mu$ -type coupling, squared in order parameter and linear in strain.^{11,14} However, it is difficult to see a Landau-Khalatnikov maximum (associated with the Edwards-Anderson order parameter in this case) (Ref. 10) above such a strong fluctuation background. Taking into account earlier dielectric permittivity $\epsilon_{11}(T)$ results which showed a deviation from the Curie-Weiss law below 140 K,⁶ we conclude that neither FE nor AFE ordering but rather the local structural competition mechanism (between FE and AFE orderings) is the origin of this strong broad damping anomaly centered near 120 K. Since the fluctuations usually indicate a random force resulting from the substitutional disorder,¹¹ the difference

of damping behavior between DRADA-0.28 and DRADA-0.10 also implies that this random force is stronger in the $x = 0.28$ crystal.

IV. CONCLUSIONS

From the fits of Eq. (2) to the high-temperature frequency shifts, we obtain the zero-temperature bare phonon frequency $\omega_a(0, x)$, Debye temperature $\Theta(x)$, and the anharmonicity coefficient $A(x)$. The tendencies for Θ and $\omega_a(0, x)$ are to increase from the DRDA side to the DADA side, as can be expected in view of the higher frequency of the modes on the DADA-rich side. The anharmonic factors also increase with higher ND_4 content and are smaller than those in the RADP system.^{8,9,20}

A main feature of the acoustic phonon spectra in DRADA ($x = 0, 0.10, \text{ and } 0.28$) for LA[100] phonons is that the frequency shift shows a positive (hardening) instead of a negative coupling contribution (softening) at the phase transition. The sign of the coupling contribution may be related to the temperature responses of lattice parameters $a(T)$ and $c(T)$. A smaller lattice constant is usually associated with a stiffer interatomic force constant and implies a contraction Δa which leads to the LA[100] phonon hardening. However, the measurements we performed on pure DRDA for LA[001] (c -axis) phonons, not reported here, revealed a negative contribution at the FE transition temperature. This may be related to the expansion Δc observed in the related crystal KH_2PO_4 just below T_c .¹³

From the temperature dependences of damping in DRADA-0.10 and DRADA-0.28, we conclude qualitatively that order-parameter fluctuations grow and become the major dynamic damping mechanism over a wide temperature range as ND_4 concentration increases. By comparing with the NMR and dielectric results, it is concluded that the local structural competition between FE ordering and AFE ordering tendencies is responsible for these broad acoustic damping anomalies in DRADA-0.10 and DRADA-0.28. A Landau-Khalatnikov damping peak associated with actual FE ordering appears in DRDA and as a second peak in DRADA-0.10.

ACKNOWLEDGMENTS

The authors express sincere thanks to Dr. N. J. Pinto and Dr. Z. Trybula for crystal growth, to Dr. I. G. Siny and Greg Pastalan for their earlier technical assistance and to Professor George F. Tuthill for helpful theoretical discussions. This work was supported in part by NSF Grant No. DMR-9017429 and DOE Equipment Grant No. FG05-91ER79046.

¹V. H. Schmidt, S. Waplak, S. Hutton, and P. Schnackenberg, Phys. Rev. B **30**, 2795 (1984).

²E. Courtens, J. Phys. Lett. (Paris) **43**, L199 (1982).

³Z. Trybula, V. H. Schmidt, J. E. Drumheller, D. He, and Z. Li,

Phys. Rev. B **40**, 5289 (1989).

⁴C.-S. Tu, V. H. Schmidt, and A. A. Saleh, Phys. Rev. B **48**, 12 483 (1993).

⁵F. L. Howell, N. J. Pinto, and V. H. Schmidt, Phys. Rev. B **46**,

- 13 762 (1992).
- ⁶N. J. Pinto, Ph.D. thesis, Montana State University, 1992.
- ⁷N. J. Pinto, K. Ravindran, and V. H. Schmidt, *Phys. Rev. B* **48**, 3090 (1993).
- ⁸E. Courtens, R. Vacher, and Y. Dagorn, *Phys. Rev. B* **33**, 7625 (1986).
- ⁹E. Courtens, R. Vacher, and Y. Dagorn, *Phys. Rev. B* **36**, 318 (1987).
- ¹⁰E. Courtens, F. Huard, and R. Vacher, *Phys. Rev. Lett.* **55**, 722 (1985).
- ¹¹W. Rehwald, *Adv. Phys.* **22**, 721 (1973).
- ¹²Z. M. Liu, Ph.D. thesis, Montana State University, 1990.
- ¹³Landolt-Bornstein, New Series, Vol. III/16b, edited by K.-H. Hellwege (Springer, Berlin, 1982).
- ¹⁴T. Hikita, P. Schnackenberg, and V. H. Schmidt, *Phys. Rev. B* **31**, 299 (1985).
- ¹⁵H. G. Danielmeyer, *J. Acoust. Soc. Am.* **47**, 151 (1970).
- ¹⁶C. Kittel, *Introduction to Solid State Physics*, 5th ed. (Wiley, New York, 1976), p. 137.
- ¹⁷*Handbook of Mathematical Functions*, 7th printing, edited by M. Abramowitz and I. A. Stegun (Dover, New York, 1970), p. 998.
- ¹⁸P. Bonnet, M. Boissier, C. Vedel, and R. Vacher, *J. Phys. Chem. Solids* **44**, 515 (1983).
- ¹⁹N. J. Pinto, F. L. Howell, and V. H. Schmidt, *Phys. Rev. B* **48**, 5983 (1993).
- ²⁰A. Bouchalkha, Z. Pan, and J. P. Wicksted, *Phys. Rev. B* **44**, 12 016 (1991).